Modification of the Microstructure in Poloxamer Block Copolymer−Water−"Oil" Systems by Varying the "Oil" Type

Peter Holmqvist,[†] Paschalis Alexandridis,*[,†,‡] and Björn Lindman[†]

Physical Chemistry 1, Center for Chemistry and Chemical Engineering, Lund University, S-221 00 Lund, Sweden, and Department of Chemical Engineering, State University of New York at Buffalo, Buffalo, New York 14260-4200

Received May 6, 1997; Revised Manuscript Received September 3, 1997[⊗]

ABSTRACT: Amphiphilic block copolymers can self-assemble in the presence of selective solvents ("water" and "oil") into a variety of different microstructures. The role that "oil" plays in the phase behavior and structure of copolymer−oil−water systems is the focus of the present investigation. We examined a poloxamer-type poly(ethylene oxide)−poly(propylene oxide)−poly(ethylene oxide) triblock copolymer (Pluronic F127: $E_{100}P_{70}E_{100}$) in ternary isothermal systems with water and each of three "oils" (of varying polarity), *p*-xylene, *n*-butyl acetate and butan-1-ol. A total of six phases with different microstructures have been identified in the ternary systems studied here: normal (oil-in-water) micellar cubic (I_1), normal hexagonal (H_1), lamellar (L_α), and reverse (water-in-oil) hexagonal (H_2) lyotropic liquid crystals, and normal micellar (L_1) and reverse micellar (L_2) solutions. The number and types of phases, as well as the composition range of their stability, are different for each ternary system, reflecting the effects of oil. Systematic small-angle X-ray scattering (SAXS) measurements have been performed in order to establish the structure of the phases and determine their characteristic length-scales. The location of the "oils" in the different self-assembled microstructures has been deduced from the structural dimensions obtained from SAXS and the constraints imposed by the copolymer total volume fraction and interfacial area: all xylene is present in the interior (apolar core) of the oil-in-water microdomains and butanol is located at the interfacial region between poly(propylene oxide) and poly(ethylene oxide), while butyl acetate contributes to both the core and the interfacial domains.

Introduction

The phase behavior and structure of amphiphilic block copolymers in selective solvents ("water" and "oil") are the subject of an ongoing investigation in our group.[1−8] In particular, we have studied the self-assembly (in binary and ternary systems with solvents) of a number of poloxamer-type block copolymers having the composition/block sequence $E_xP_nE_x$, where E denotes poly(ethylene oxide) and P, poly(propylene oxide). We have also reported recently ternary phase diagrams for triblock copolymers with a more hydrophobic middle block, poly(1,2-butylene oxide), denoted here as B, or poly(*n*-butylene oxide) = poly(tetrahydrofuran), denoted T.[4,8] In addition to forming micelles in aqueous solution, $E_xP_nE_x$ and $E_xB_nE_x$ triblock copolymers can self-assemble into lyotropic liquid crystalline structures, having one- (lamellar), two- (cylindrical), or three-dimensional (cubic) order, "normal" (oil-in-water) or "reverse" (water-in-oil) morphology, and discrete (e.g., spheres) or continuous (e.g., interconnected bilayer) topology, depending on the ternary copolymer−water−oil composition.[1−13] A number of practical applications take advantage of the rich structural polymorphism exhibited by macromolecular amphiphiles, often without adequate knowledge of the underlying phase behavior and structure.[14−17] Our work provides such needed fundamental knowledge, and lays groundwork for improved and novel applications.

The different phases formed in ternary amphiphilic block copolymer−oil−water systems are comparable to, but of much greater variety than those reported for surfactant−oil−water systems.[4,18,19] The self-assembly of amphiphilic block copolymers in selective solvents resembles in many respects, that of block copolymers in the bulk ("dry") state. In the latter case, the formation of structure (order) requires a certain degree of segregation between the blocks (which depends on block−block interaction and block size), while the type of structure depends on the volume fraction of the different blocks.[20,21] In the case of block copolymers in selective solvents, we found the type of structure to depend not only on the volume fraction of the different blocks but also on the volume fraction of the respective solvents.[1−4]

An important issue in our understanding and control of self-assembly has to do with how the nature of the oil present affects the phase behavior and structure afforded by the amphiphilic block copolymers. The oil swells to a varying degree the hydrophobic blocks of the macromolecular amphiphile, and thus its selection will be of great importance in modulating the interfacial "curvature". The effects of oil on the self-assembled microstructure is a topic which has not been addressed so far in the literature, and it forms the basis of the present investigation.

The work described here focuses on the isothermal phase behavior and structure of ternary systems based on the $E_{100}P_{70}E_{100}$ (Pluronic F127) copolymer and containing water and "oil". Pluronic F127 is a relatively long and hydrophilic (consists of 70 wt % E) amphiphile which has been known for long time to form a "gel" in the presence of water, at copolymer concentrations as low as 20 wt %.[9,11,14,15,22−24] This "gel" (a micellar cubic phase, as was recently determined) is thermoreversible and finds interesting biomedical applications, e.g., in hydrophobic drug solubilization and release; $E_{100}P_{70}E_{100}$ is also used for the stabilization of water/oil emulsions.[15] Despite these applications, very little fundamental work had been published on the self-assembly of $E_{100}P_{70}E_{100}$. We have examined three solvents: *p*-xylene, which we

* To whom correspondence should be addressed at the State University of New York. E-mail: palexand@eng.buffalo.edu.
† Lund University.
‡ State University of New York at Buffalo.
⊗ Abstract published in *Advance ACS Abstracts,* October 1, 1997.

S0024-9297(97)00625-6 CCC: $14.00

have previously[1,2] shown to be a selective solvent for the P block, *n*-butyl acetate, which is promoted as an environmentally friendly replacement of xylene,[25] and butan-1-ol, which is comparable in terms of molecular structure to the P monomers (and thus expected to be a good solvent for them) but is also interfacially active in water.[26] We chose to work with "oils" which differ in polarity but are comparable in terms of density and molecular weight.

The role of the "oils" on the ternary phase behavior and structure is discussed in this paper. The location of the different "oils" in the microdomains of the various structures was ascertained with the help of systematic small-angle X-ray scattering (SAXS) measurements. The results and discussion section is organized in the following manner: First we examine the overall phase behavior of the ternary isothermal phase diagrams formed by the three different "oils". We then present the structural characterization of the one-phase regions. The next section probes the location of the "oil" in the self-assembled microstructure. The observations from our phase behavior and SAXS studies are discussed in terms of role of "oil" in modifying the microstructure.

Materials and Methods

Materials. The Pluronic F127 poly(ethylene oxide-*b*-propylene oxide-*b*-ethylene oxide) copolymer, denoted here $E_{100}P_{70}E_{100}$ [based on its molecular weight of 12 600 and 70% poly(ethylene oxide) composition]. was kindly supplied by BASF Corp., and was used as received. Butan-1-ol was purchased from BDH Chemicals Ltd (Poole, England), *n*-butyl acetate was obtained from E. Merck (Damstadt, Germany), and *p*-xylene (1,4-dimetylbenzene) of purity >99.0% was supplied from Fluka Chemie AG, Switzerland. Millipore-filtered water was used for all preparations. The bulk density of the $E_{100}P_{70}E_{100}$ block copolymer is 1.05 g/mL at 25 °C according to the manufacturer. The bulk densities of *p*-xylene, *n*-butyl acetate, butan-1-ol and water are 0.86, 0.88, 0.81, and 1.0 g/mL, respectively.

Phase Diagram Determination. In order to determine the location and boundaries of the different phases on the ternary phase diagram, a large number of samples in each system, covering the whole range of copolymer−"oil"−water compositions, were individually prepared in glass tubes, which were flame-sealed, homogenized, and left to equilibrate at 25 °C for at least 2 weeks. Following equilibration, the samples were checked for phase separation and birefringence. The one-phase samples were clear and macroscopically homogeneous; the two- (or three-) phase samples were either homogeneous but opaque/milky-white or were macroscopically heterogeneous/phase-separated. Inspection of the samples under polarised light was used to detect birefringence. This distinguishes between the isotropic (nonbirefringent) micellar solutions or cubic liquid crystals and the anisotropic (birefringent) lamellar or hexagonal liquid crystals.[6,9] More samples were prepared in the vicinity of the phase boundaries in order to accurately determine their location. Representative samples were examined repeatedly (over the course of a few months) to ensure that the structures attained were in a thermodynamic equilibrium state.

Small-Angle X-ray Scattering (SAXS). Small-angle X-ray scattering was used to determine the structure (and occasionally the boundaries) of the lamellar, hexagonal, and cubic lyotropic liquid crystalline phases. The measurements were performed on a Kratky compact small-angle system equipped with a position sensitive detector (OED 50M from MBraun, Graz, Austria) containing 1024 channels of 51.3 μm width. Cu Kα radiation of wavelength 1.542 Å was provided by a Seifert ID300 X-ray generator, operating at 50 kV and 40 mA. A 10 μm thick nickel filter was used to remove the Kβ radiation, and a 1.5 mm tungsten filter protected the detector from the primary beam. The sample-to-detector distance was 277 mm. The volume between the sample and the detector was kept under vacuum during data collection in order to minimize the background scattering. The temperature was kept constant at 25 °C (± 0.1 °C) with a Peltier element. The obtained Bragg diffraction peaks are relatively sharp, and we thus used the slit-smeared SAXS data in our evaluation.[1,6] All samples examined by SAXS were one-phase and had been equilibrated for at least a month before the measurement.

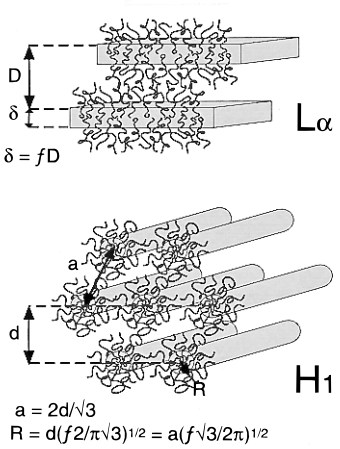

Figure 1. Schematic representation of the self-organization of the amphiphilic block copolymers into the lamellar and normal hexagonal structures, indicating the different characteristic lengths. Here D is the lattice spacing between two adjacent lamellar layers, δ is the apolar thickness of a lamella, d is the distance between adjacent rows of cylinders in the hexagonal structure, and R is the apolar radius of a cylinder. The shaded areas represent the apolar domains. The amphiphiles are localized at the polar/apolar interfaces. For reasons of clarity, only the copolymer molecules at the cross section of the (planar and cylindrical) assemblies are depicted, and only sections of the lyotropic liquid crystals are shown.

Structural Characterization. The structure [e.g., lamellar (smectic) or hexagonal (cylindrical copolymer assemblies crystallised in a hexagonal lattice)] of the lyotropic liquid crystalline phases was ascertained from the relative positions of the SAXS diffraction peaks on the scattering vector (q) axis. For the lamellar structure, the relative (with respect to the first and most intense peak) position of the peaks should obey the relationship $1 \div 2 \div 3 \div ...$, while for the hexagonal structure the expected relationship is $1 \div \sqrt{3} \div 2 \div \sqrt{7} \div ....$[27] The lattice spacing in the lamellar and hexagonal structures (see schematic of Figure 1) was determined from the position (q^*) of the first diffraction peak, using the following formulas:

$$\text{lamellar} \qquad q^* = \frac{2\pi}{D} \tag{1}$$

$$\text{hexagonal} \qquad q^* = \frac{2\pi}{d} \tag{2}$$

D is the spacing between two adjacent layers in the lamellar structure and d is the distance between adjacent rows of cylinders in the hexagonal structure (see Figure 1).

From the lattice spacing between the lamellar layers and the cylinder rows determined above, it is possible to calculate the characteristic lengths of the hydrophobic (apolar) part of the microdomains, i.e., the apolar lamellar thickness, δ, and the apolar cylinder radius, R (see Figure 1), using the following expressions:

$$\delta = fD \tag{3}$$

$$R = \sqrt{\frac{2f}{\pi\sqrt{3}}}\, d \tag{4}$$

f is the volume fraction of the apolar components at a given copolymer−oil−water composition (the assumption of a sharp interface between the polar and apolar domains is implicit in the above equations). The definition of the apolar volume fraction for the different "oils" is discussed in the section immediately following.

The lamellar periodicity (lattice spacing, D) is equal to the ratio between the total volume (V) and area (A_b) of the interfacial layer. That leads to the following expression used to calculate the average area, a_p, occupied by one poly(ethylene oxide) block of a copolymer molecule at the polar/apolar interface in the lamellar structure (the interfacial area per copolymer molecule is $2a_p$):

$$a_p = \frac{1}{D}\left(\frac{v_p}{\Phi_{int}}\right) \quad (5)$$

Φ_{int} is the volume fraction of the components participating at the polar/apolar interface, and v_p is the volume of one block copolymer molecule (≈20 000 Å^3 for F127).

The expression used to calculate the interfacial area per poly(ethylene oxide) block in the normal (oil-in-water) hexagonal structure is

$$a_p = \frac{\sqrt{f\pi\sqrt{3}}}{\sqrt{2}d}\left(\frac{v_p}{\Phi_{int}}\right) \quad (6)$$

Equation 6 is obtained by setting the (apolar) volume-to-area ratio for the case of infinite cylinders ($fv_p/\Phi_{int}a_p$) equal to the apolar cylinder radius of eq 4.[1,2,4] In the case of a reverse (water-in-oil) hexagonal structure, f in Equation 6 is replaced by the polar volume fraction, $1 - f$.

Apolar and Interfacial Volume Fractions. The relative volume fraction of the polar and apolar regions in the microstructure must be defined first, in order to calculate the interfacial area per block copolymer and the apolar thickness and apolar radius of the microdomains in the lamellar and hexagonal regions, respectively. The apolar volume fraction, f, will certainly include the hydrophobic poly(propylene oxide) block (which in the case of $E_{100}P_{70}E_{100}$ constitutes about 30% of the copolymer volume) and also all or part of the "oil" present in the ternary system:

$$f = \Phi_{PPO} + x\Phi_{oil} \quad (7)$$

Φ_{PPO} is the volume fraction of poly(propylene oxide) in the ternary copolymer−oil−water system, Φ_{oil} is the total volume fraction of "oil", and x is the fraction of this "oil" which is located in the apolar part of the self-assembled microdomains.

The interfacial volume fraction Φ_{int} is defined in an analogous way. We consider all the block copolymer to be interfacially active (and its volume fraction to be the major constituent of the interfacial volume fraction); part of the "oil" could also be located at the polar/apolar interface. Similarly to the apolar volume fraction, the interfacial volume fraction is given by

$$\Phi_{int} = \Phi_p + n\Phi_{oil} \quad (8)$$

Φ_p is the total volume fraction of the copolymer and n is the fraction of the "oil" volume fraction, Φ_{oil}, which is located at the polar/apolar interface.

The location of the "oil" in the microstructure will affect the value of both Φ_{int} and f. Assuming different locations of the "oil" in the microdomains, it is possible to calculate the different characteristic lengths and then check this assumption against the trends expected for these characteristic parameters. The estimation of Φ_{int} and f will be presented in detail in section C of the Results and Discussion.

Results and Discussion

A. Phase Behavior. Overview. The phase diagrams of $E_{100}P_{70}E_{100}$ with water and the three different "oils" are shown in Figure 2. The phase diagrams for the ternary $E_{100}P_{70}E_{100}$−xylene−water and $E_{100}P_{70}E_{100}$−butyl acetate−water systems at 25 °C are presented here for the first time; the $E_{100}P_{70}E_{100}$−butanol−water phase diagram has been reported in detail in our previous work.[8] The following general trends are observed in all three phase diagrams: The block co-

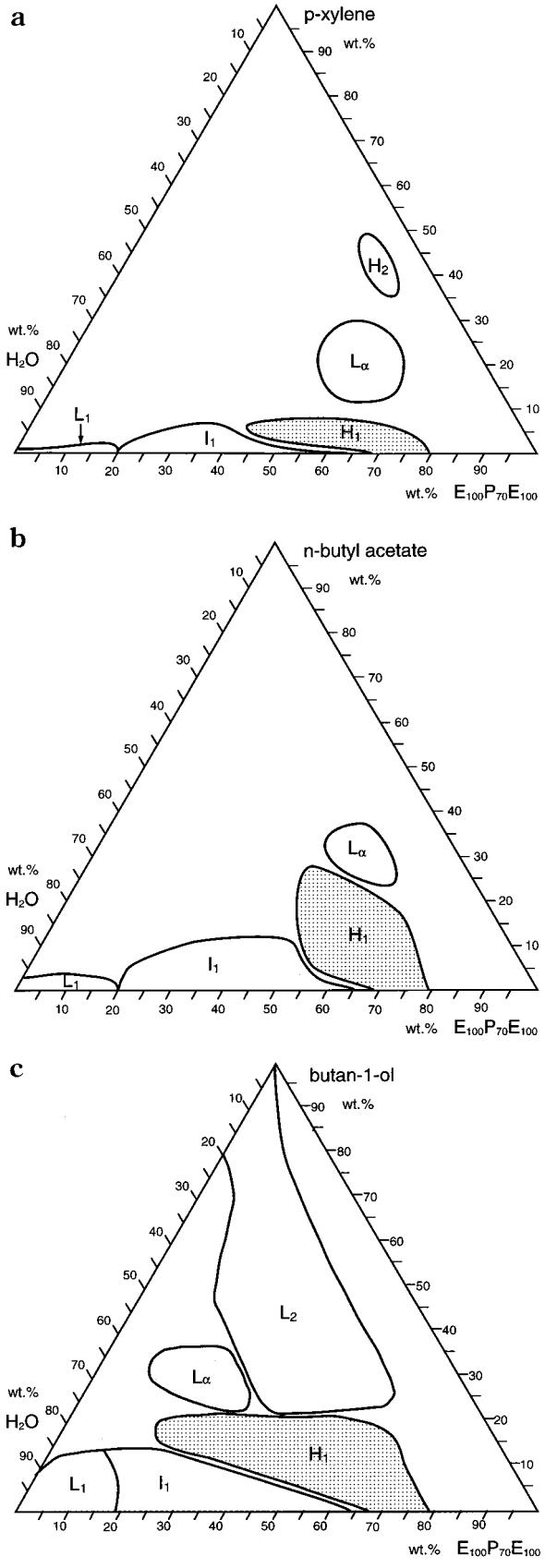

Figure 2. (a) Phase diagram of the $E_{100}P_{70}E_{100}$−*p*-xylene−water system at 25 °C. (b) Phase diagram of the $E_{100}P_{70}E_{100}$−*n*-butyl acetate−water system at 25 °C. (c) Phase diagram of the $E_{100}P_{70}E_{100}$−butan-1-ol−water system at 25 °C. The following notation is used in all three phase diagrams: L_1 denotes the water-rich (micellar) solution region, I_1 the normal ("oil"-in-water) micellar cubic liquid crystalline region, H_1 the normal hexagonal region, H_2 the reverse hexagonal region, L_α the lamellar region, and L_2 the alkanol-rich (reverse micellar) solution region.

polymer forms micelles in water at a high water content; when the volume fraction of the copolymer is sufficiently high (≈20 wt %) the micelles order in a cubic lattice (micellar cubic region). At higher copolymer concentrations, along the copolymer−water axis, the curvature changes (in order to accommodate the Φ_{PPO} volume fraction which becomes too large to be "enclosed" in the spherical domains of the micellar cubic phase) and the cubic micellar structure changes to a hexagonal structure (cylindrical domains). No other phases are formed along the copolymer−water binary axis, but a lamellar phase is found in all three ternary systems in the presence of "oil". Furthermore, a reverse (water-in-oil) hexagonal region was found in the xylene system and a water-lean (reverse micellar) solution region was found in the butanol system.

The progression of structures over the phase diagram, micellar solution (L_1) → micellar cubic (I_1) → hexagonal (H_1) → lamellar (L_α) → reverse hexagonal (H_2) (only in the xylene system) → reverse micellar solution (L_2) (only in the butanol system), reflects a change in the interfacial curvature with increasing oil/water composition ratio.[4,28]

$E_{100}P_{70}E_{100}$−*p*-Xylene−Water, $E_{100}P_{70}E_{100}$−*n*-Butyl Acetate−Water and $E_{100}P_{70}E_{100}$−Butan-1-ol−Water Systems: Different Phases and Their Composition Range. The isotropic solution region, denoted L_1, is stable along the $E_{100}P_{70}E_{100}$−water axis up to 20 wt % copolymer and can dissolve almost 15 wt % butanol but less than 5 wt % butyl acetate or xylene. The L_1 samples are optically transparent and fluid, but they progressively become more viscous as the copolymer concentration increases.

A region where the structure is cubic and consists of discrete micelles is formed at 20 wt % copolymer along the $E_{100}P_{70}E_{100}$−water axis and continues all the way up to 65 wt % copolymer. This region, denoted I_1, dominates the copolymer−water binary axis and can dissolve up to 13 wt % butanol or butyl acetate, but only 7−8 wt % xylene. In our study of the $E_{100}P_{70}E_{100}$−butanol−water system, we have shown that the I_1 region has a primitive cubic structure.[8] The wide range of copolymer concentrations where the cubic structure is stable is notable; it is very uncommon to have a micellar cubic phase all the way up to 65 wt % surfactant.[18]

A birefringent (anisotropic) region of hexagonal structure, denoted H_1, supersedes the I_1 region, and is stable along the copolymer-water axis at 70−80 wt % $E_{100}P_{70}E_{100}$. H_1 is remarkable in its ability to swell with all the "oils" examined, xylene, butyl acetate, and butanol, and in its stability over a wide range of compositions. The extent of the H_1 region inside the ternary phase diagram (away from the copolymer−water axis) depends strongly on the type of "oil" present. In the butanol and butyl acetate cases the H_1 region can accommodate up to 20 wt % "oil", while it phase-separates before 10 wt % xylene can be added. In the butanol system, the H_1 region is swelling all the way down to 18 wt % $E_{100}P_{70}E_{100}$, while it only extends down to 45 wt % $E_{100}P_{70}E_{100}$ in the butyl acetate and xylene systems. The H_1 samples in all three systems are optically transparent.

Another birefringent phase (denoted L_α), of lamellar structure, was identified in all three systems, in the presence of "oil". The L_α phase is stable at around 20 wt % $E_{100}P_{70}E_{100}$ and 20 to 35 wt % butanol, while it is formed at a much higher block copolymer concentration, 55 wt % $E_{100}P_{70}E_{100}$, in the butyl acetate (25−40 wt % butyl acetate) and xylene (15−30 wt % xylene) systems. In the butanol and butyl acetate systems, the lamellar regions could not be readily distinguished from the hexagonal regions by macroscopic ocular means, because of the narrow two-phase region and similar refractive indices. In this case, the L_α phase boundary with the hexagonal region (together with the L_α structure) was determined with the aid of SAXS measurements. The L_α samples are optically transparent.

Finally, one more birefringent phase is exhibited in the $E_{100}P_{70}E_{100}$−xylene−water system at 50 wt % copolymer and at low (≈10 wt %) water contents. This phase was determined to be reverse (water-in-oil) hexagonal (H_2). No such H_2 phase was detected at 25 °C for the butyl acetate and butanol systems.

In the $E_{100}P_{70}E_{100}$−butanol−water system an extensive water-lean solution region (L_2) was found at high "oil" concentrations. L_2 did not form in the other two systems. The L_2 samples are as fluid as the "oil" down to approximately 50 wt % "oil", and they become more viscous as the "oil" content decreases further. From SAXS measurements done in the $E_{100}P_{70}E_{100}$−butanol−water system, we observed an increasing order in the system with butanol content decreasing below 50 wt %.[8]

Effect of Oil on Phase Behavior: Comparison of the Phase Diagrams Obtained with the Three Different "Oils". Comparison of the $E_{100}P_{70}E_{100}$ ternary phase diagrams (shown in Figure 2) prepared with the three different "oils" leads to the following important observations. The L_1, I_1, and H_1 phases, all of the "oil"-in-water topology, swell with increasing amounts of "oil" when butyl acetate or butanol are used instead of (the more hydrophobic) xylene. This can only be partly attributed to the finite solubility of butyl acetate or butanol in water, because, as we will discuss in sections B and C, there are additional effects by these solvents on the lattice spacing (which is related to the swelling of the copolymer chains).

Such effects are evident, e.g., in the pronounced ability of the H_1 phase to accommodate water and oil and in the stability of the L_α region at considerably low copolymer contents, observed in the butanol system. The H_1 region in the butanol system extends down to 18 wt % $E_{100}P_{70}E_{100}$, while, for the other two "oils", H_1 only goes down to ≈45 wt % $E_{100}P_{70}E_{100}$. The butanol lamellar region is stable at low (down to 10 wt %) $E_{100}P_{70}E_{100}$ concentrations while the other two lamellar phases are found at relatively high (50−60 wt %) $E_{100}P_{70}E_{100}$ concentrations. The presence of an extended L_2 solution region in the butanol phase diagram is another indication of the significant influence of butanol has on the copolymer self-assembly.

The change of the "oil" from xylene and butyl acetate to butanol appears to increase the effective length of the copolymer molecules so that they can stabilize (in the absence of long-range electrostatic interactions) liquid crystalline self-assemblies at low copolymer concentration and thus over longer interaggregate distances. The analysis (presented in section C) of systematic SAXS measurements, performed in the H_1 and L_α regions (which are common to all three phase diagrams and extend over a wide range of copolymer−oil−water compositions), enabled us to get a firmer grip on the role of the "oil" on the microstructure.

B. Structural Characterization of the Hexagonal and Lamellar Regions. The $E_{100}P_{70}E_{100}$−*p*-Xylene−Water System. Three different birefringent regions have been observed in this system; SAXS diffraction patterns representative of each region are shown in Figure 3. Diffraction peaks with relative positions of $1 \div \sqrt{3} \div \sqrt{7} \div 3$ can be seen in Figure 3a,

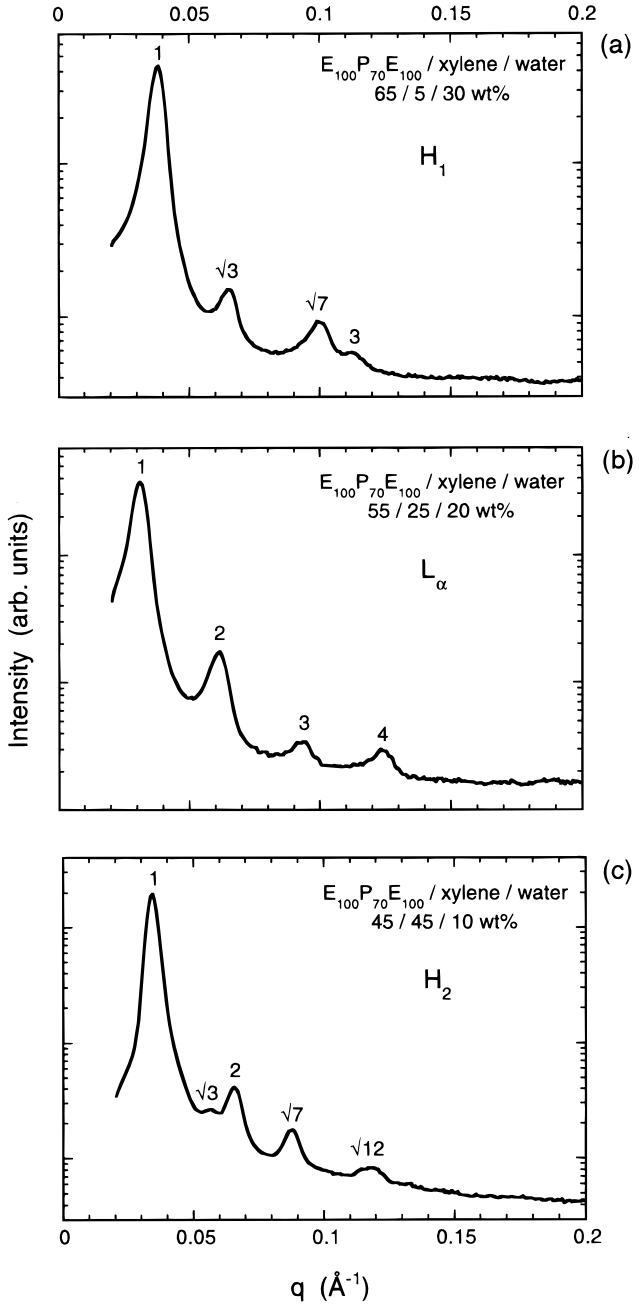

Figure 3. SAXS diffraction patterns from representative samples in (a) the normal hexagonal, (b) the lamellar, and (c) the reverse hexagonal lyotropic liquid crystalline regions of the $E_{100}P_{70}E_{100}$–*p*-xylene–water phase diagram. The sample compositions are 65/5/30, 55/25/20, and 45/45/10 wt % $E_{100}P_{70}E_{100}$/xylene/water, respectively.

indicating that this sample has a hexagonal structure. Since this hexagonal region is located between the normal micellar cubic and the lamellar regions in the phase diagram, its morphology should be normal (oil-in-water). In the SAXS diffraction pattern of Figure 3b, obtained from a sample in the birefringent region adjacent to the H_1 phase, peaks with the relative positions of $1 \div 2 \div 3 \div 4$ were found, which indicate a lamellar structure. A typical SAXS diffraction pattern from the third birefringent phase (at low water content) is presented in Figure 3c. The peaks follow the pattern expected from a hexagonal structure, with relative positions of $1 \div \sqrt{3} \div 2 \div \sqrt{7} \div \sqrt{12}$. According to its location in the phase diagram (at higher oil content than the L_α) this phase is identified as reverse (water-in-oil) hexagonal. SAXS lattice spacings are presented in Table 1 (for the normal hexagonal region) and Table 2 (for the lamellar region) and on the phase diagram section shown in Figure 5.

The $E_{100}P_{70}E_{100}$–*n*-Butyl Acetate–Water System. Several SAXS measurements have been carried out in the birefringent regions of this phase diagram to establish the different structures (H_1 and L_α). The SAXS measurements also helped in the delineation (to a 3% accuracy) of the phase boundary between the H_1 and L_α regions. A typical SAXS diffraction pattern at 20 wt % butyl acetate content is presented in Figure 4a. Diffraction peaks at the relative positions of $1 \div \sqrt{3} \div \sqrt{7} \div \sqrt{12}$ can be discerned. These are some of the characteristic peaks expected for a hexagonal structure (the peaks at positions 2 and 3 are missing, for reasons which are not clear to us at this time). A SAXS diffraction pattern from a sample with higher (30 wt %) butyl acetate concentration is presented in Figure 4b. Peaks following the relative positions of $1 \div 2 \div 3$, characteristic of lamellar spacing, can be seen. The distances between adjacent lamellae (D) and rows of cylinders (d) were calculated using eqs 1 and 2, respectively. These values are presented in Table 1 (for the hexagonal region) and Table 2 (for the lamellar region) and on the phase diagram section of Figure 5.

The $E_{100}P_{70}E_{100}$–Butan-1-ol–Water System. A detailed description of the structural characterization of the $E_{100}P_{70}E_{100}$–water–butanol system has been reported elsewhere.[8] The lattice spacings obtained from SAXS measurements are presented in this paper, in order to facilitate comparison to the lattice spacing obtained from the other two "oils". The characteristic dimensions are presented in Table 1 (hexagonal region) and Table 2 (lamellar region) and are also indicated on the phase diagram section shown in Figure 5.

SAXS Lattice Spacing Trends. Lattice spacings obtained directly (i.e., no assumptions involved) from the SAXS experiments are presented in Figure 5, at the respective sample compositions in sections of the three phase diagrams with butanol, butyl acetate, and xylene. The SAXS lattice spacings in the normal hexagonal and lamellar phases decrease with increasing copolymer concentration at constant "oil" content in all three systems. This observation can be explained as follows: for a given structure, when the copolymer content increases, the number of lamellae/cylinders must increase in order to accommodate the increased amount of copolymers, and as a result the spacing between the lamellae/cylinders in the structure will decrease.

A comparison of the lattice spacing values at the same copolymer–water–"oil" composition in the different phase diagrams leads to the notable observation that the SAXS spacing is decreasing as the "oil" is getting more polar (and less apolar), i.e., from xylene to butyl acetate to butanol. This trend is followed both in the normal hexagonal and in the lamellar regions. It becomes apparent from this observation that the oil is affecting the effective length of the copolymer molecules.

Considering that the interfacial area per copolymer molecule should be invariant of the structure where it is located (as reported in ternary systems of PEO-containing nonionic surfactants[19] and as we have observed in a number of poloxamer–xylene–water systems[1–5]), the observation of different lattice parameters for the three different solvents at comparable compositions in the phase diagram suggested to us that the assumptions (i) of only the copolymer being inter-

Table 1. Values for Lattice Spacing, Area per PEO Block at the Polar/Apolar Interface, a_p, and Apolar Cylinder Radius, R, at Various Compositions in the Normal Hexagonal Region of the Three $E_{100}P_{70}E_{100}$−"oil"−Water Ternary Systems[a]

wt % polymer $E_{100}P_{70}E_{100}$	wt % water	wt % *p*-xylene	wt % *n*-butyl acetate	wt % butanol	lattice spacing (Å)	a_p (Å^2) [f_1 and Φ_1]	R (Å) [f_1]	a_p (Å^2) [f_3 and Φ_3]	R (Å) [f_3]	a_p (Å^2) [f_2 and Φ_2]	R (Å) [f_2]	molar ratio H_2O/EO segment	molar ratio oil/copolymer
70	30			0	151.4					143.7	41.8	1.6	0
55	40			5	149.2					154.3	37.5	2.7	16.3
60	35			5	143.7					154.1	37.7	2.2	15.0
70	25			5	134.8					153.1	38.1	1.3	12.8
40	50			10	143.7					170.0	32.4	4.6	44.9
45	45			10	141.1					166.0	33.5	3.7	39.9
50	40			10	138.6					162.4	34.4	3.0	35.9
55	35			10	138.6					156.6	35.9	2.4	32.7
65	25			10	129.8					156.4	36.2	1.4	27.7
70	20			10	127.9					154.0	36.9	1.1	25.7
25	60			15	154.6					167.9	30.5	8.9	107.8
30	55			15	146.4					169.4	30.8	6.8	89.7
35	50			15	141.4					168.1	31.4	5.3	77.0
40	45			15	136.5					167.4	31.9	4.2	67.4
44	41			15	136.5					162.5	33.2	3.4	61.3
50	35			15	131.0					162.4	33.5	2.6	53.9
55	30			15	131.1					157.1	34.9	2.0	49.0
60	25			15	127.9					156.2	35.3	1.5	44.9
65	20			15	123.9					156.6	35.4	1.1	41.5
20	60			20	161.2					155.5	31.9	8.1	143.8
25	55			20	153.9					156.3	31.3	10.5	170.3
30	50			20	144.7					159.9	31.7	6.2	119.8
35	45			20	137.7					162.0	31.8	4.8	102.7
40	40			20	130.3					165.4	31.5	3.7	89.9
45	35			20	126.1					165.4	31.8	2.9	79.9
50	30			20	130.3					155.3	34.2	2.2	71.9
65	25		10		168.9			130.9	49.1			1.4	17.4
55	30		15		187.0			126.3	53.0			2.0	30.9
65	20		15		145.1			151.1	43.8			1.2	26.5
45	35		20		172.6			147.5	47.6			3.0	50.8
55	25		20		161.5			133.6	48.0			1.7	43.8
45	30		25		187.0			133.6	54.0			2.5	64.8
45	50	5			183.7	179.8	48.5					4.1	13.9
55	40	5			182.1	159.0	51.7					2.7	11.4
65	30	5			165.3	157.3	50.1					1.7	9.7

[a] The lattice spacing is obtained directly from SAXS measurements, while in the calculation of a_p and R, the values for the apolar volume fraction, f, and the interfacial volume fraction, Φ, are involved. See text for details.

Table 2. Values for Lattice Spacing, Area per PEO Block at the Polar/Apolar Interface, a_p, and Apolar Lamellar Thickness, δ, at Various Compositions in the Lamellar Region of the Three $E_{100}P_{70}E_{100}$−"Oil"−Water Ternary Systems[a]

wt % polymer $E_{100}P_{70}E_{100}$	wt % water	wt % *p*-xylene	wt % *n*-butyl acetate	wt % butanol	lattice spacing (Å)	a_p (Å^2) [Φ_1]	δ (Å) [f_1]	a_p (Å^2) [Φ_3]	δ (Å) [f_3]	a_p (Å^2) [Φ_2]	δ (Å) [f_2]	molar ratio H_2O/EO segment	molar ratio oil/copolymer
25	50			25	158.2					242.0	20.1	7.0	170.3
30	45			25	146.4					240.0	20.7	5.2	141.9
15	55			30	196.6					210.8	21.6	12.8	340.5
20	50			30	174.4					216.9	21.6	8.8	255.4
25	45			30	158.2					219.9	21.7	6.3	204.3
15	50			35	196.6					190.2	23.6	11.7	397.3
20	45			35	167.9					205.2	22.5	7.9	300.0
25	40			35	146.5					218.0	21.6	5.6	238.4
55	20		25		178.5			154.4	45.6			1.3	52.1
55	15		30		146.5			177.5	40.4			1.0	62.5
44	21		35		189.3			150.8	49.7			1.8	91.2
55	30	15			204.0	186.8	67.8					2.0	34.2
65	20	15			173.6	184.9	62.9					1.1	29.0
55	20	25			202.0	191.7	89.2					1.3	57.0

[a] The lattice spacing is obtained directly from SAXS measurements, while in the calculation of δ and a_p, the values for the apolar volume fraction, f, and the interfacial volume fraction, Φ, respectively, are involved. See text for details.

facially active and (ii) of the apolar domains consisting of the PPO segments and all the "oil", which we have used previously[1,2,4,6] to relate the lattice spacing to the system composition and to the copolymer interfacial area, have to be reconsidered.

The difference in spacing between the different oils can then be related to a change of the apolar and/or interfacial volume in the ternary system. When the oil is to some extent polar, smaller amounts of it will contribute to the volume fraction of the apolar domains. The thickness of the lamellae and cylinders will then decrease, and the number of lamellae and cylinders will increase (for the same total amount of copolymer); as a result, the spacing between them will decrease. More specific information on the relationship between the characteristic distances, and the location of the oil in the microdomains is presented immediately below.

C. Location of "Oil" in the Microstructure. The calculated values of apolar lamellar thickness, δ, apolar cylinder radius, R, and interfacial area per poly(ethylene oxide) block, a_p, depend on the values used for apolar volume fraction (f) and the interfacial volume fraction

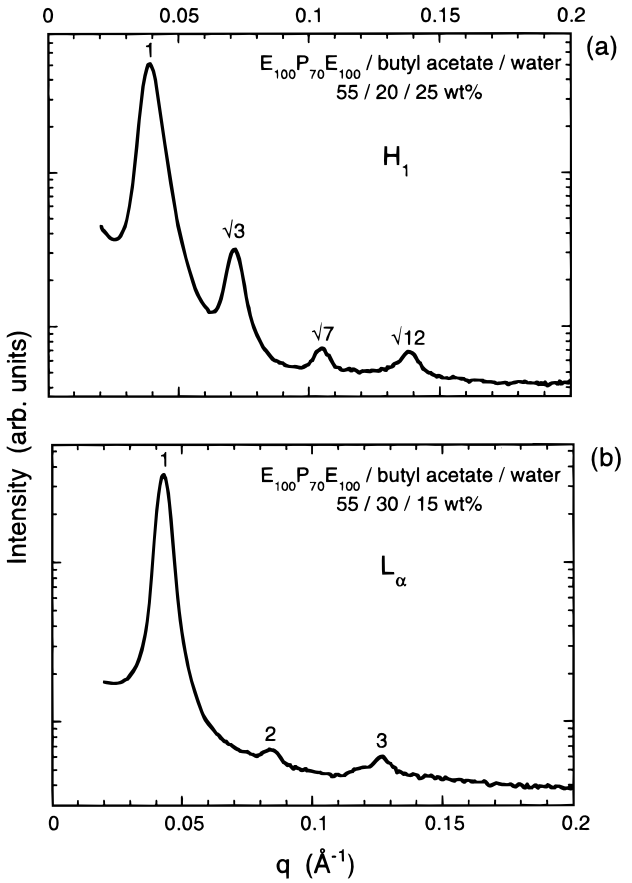

Figure 4. SAXS diffraction patterns from representative samples in (a) the normal hexagonal and (b) the lamellar lyotropic liquid crystalline region of the $E_{100}P_{70}E_{100}$−*n*-butyl acetate−water phase diagram. The sample compositions are 55/20/25 and 55/30/15 wt % $E_{100}P_{70}E_{100}$/butyl acetate/water, respectively.

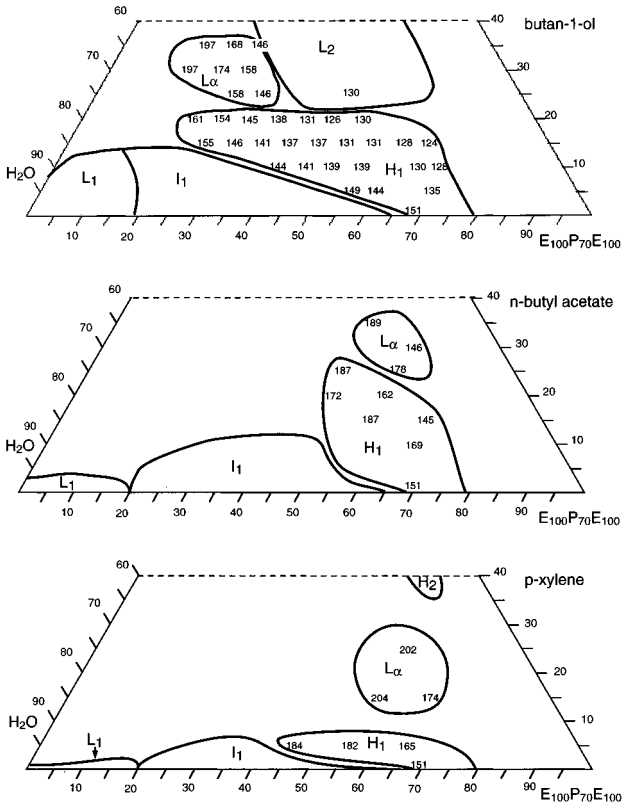

Figure 5. Lattice spacing values (Å), determined from SAXS, shown on sections of the ternary phase diagrams at the respective $E_{100}P_{70}E_{100}$/"oil"/water compositions. H_1 denotes normal hexagonal, L_α lamellar, and H_2 reverse hexagonal region. (top) $E_{100}P_{70}E_{100}$−butan-1-ol−water phase diagram; (middle) $E_{100}P_{70}E_{100}$−*n*-butyl acetate−water phase diagram; (bottom) $E_{100}P_{70}E_{100}$−*p*-xylene−water phase diagram.

(Φ_{int}), following eqs 3−6. The definitions of f and Φ_{int} could at a first glance seem straightforward, but the macromolecular nature of the amphiphile (i.e., its ability to swell) and the polarity of both PEO and PPO blocks (due to the ether oxygens) render the location of the "oil" present in the microstructure an important consideration.

Location of *p*-Xylene. First we consider the case of xylene, the most hydrophobic oil, because we have already accumulated information on ternary phase diagrams for various poloxamer block copolymers with xylene and obtained a good understanding of its role.[1−5] Xylene is almost insoluble in water (its solubility is ≈0.01%) and is a bad solvent for PEO; however, it is a good solvent for PPO homopolymer. These characteristics will favor all xylene to be located in the apolar volume fraction (f), i.e., in the core of the oil-in-water microdomains. Xylene is not interfacially active, and thus essentially no xylene is expected to partition at the polar/apolar interface. So the interfacial volume fraction (Φ_{int}) will consist of only the amphiphilic block copolymer molecules. The above considerations result in the following expressions for the apolar volume fraction (f_1) and interfacial volume fraction (Φ_1) in the $E_{100}P_{70}E_{100}$− *p*-xylene−water system:

$$f_1 = \Phi_{PPO} + \Phi_{xyl} \tag{9}$$

$$\Phi_1 = \Phi_p \tag{10}$$

Φ_{PPO} is the volume fraction of poly(propylene oxide) in the ternary system, Φ_{xyl} is the xylene volume fraction, and Φ_p is the total block copolymer volume fraction. Using these values in eqs 3−6, the characteristic parameters δ, R, and a_p were calculated and are presented in Table 1 (hexagonal region) and Table 2 (lamellar).

The interfacial area per PEO copolymer block is found in the range 160−180 Å^2 for the hexagonal region and 180−190 Å^2 for the lamellar region; a_p varies by about ±10% over the composition range examined. Although the number of composition data points available for calculating the interfacial area is not large in the present $E_{100}P_{70}E_{100}$−*p*-xylene−water system, we have observed the interfacial area per copolymer molecule to be invariant of the structure for a number of other poloxamer−xylene−water systems,[1−5] and we believe that this is an indication for a correct assignment of the polar/apolar interface (where the copolymer is located) and of the location of xylene in the core of the "oil"-in-water microdomains.

Location of Butan-1-ol. Butanol is different than xylene: it is soluble in water to some extent (7.5%)[29] and, being polar, is also able to interact with both PEO and PPO blocks. The problem is to assign the proper value to both the apolar volume fraction (f) and the interfacial volume fraction (Φ_{int}). The butanol could act as a co-surfactant and participate together with the block copolymer in stabilizing the polar/apolar interfaces. In this case, the interfacial volume fraction, Φ_2, would be

$$\Phi_2 = \Phi_p + \Phi_{but} \tag{11}$$

The next question is how much of the butanol is located in the core of the "oil"-in-water microdomains

and contributes to the apolar volume fraction, f. If butanol were acting as a co-surfactant it would mainly be located at the polar/apolar interfaces (eq 11) but still contribute to the apolar volume with its methylene groups. The apolar volume fraction (f_2) would then be

$$f_2 = \Phi_{PPO} + x\Phi_{but} \quad (12)$$

where x is the fraction of the butanol which contributes to the apolar volume.

We examined a number of possible locations for butanol (in terms of the butanol participation in the interfacial and the apolar volume, eqs 11 and 12, respectively), and tested the resulting (through eqs 5 and 6, using different Φ_2 and f_2 values) values of interfacial area against our idea that the interfacial area per copolymer molecule should be invariant of composition. Using this approach, we obtained the most consistent interfacial area values in the case where all butanol participates in the interfacial volume fraction (i.e., eq 11 is valid) and 20% of butanol (i.e., $x = 0.20$ in eq 12) contributes to the apolar volume fraction. The results from these considerations are presented in Table 1 (for the hexagonal region) and Table 2 (lamellar region).

The interfacial area per PEO block is found to be in the range 145−170 Å^2 for the hexagonal region. Again a_p varies by only about ±10% over the wide composition range examined and is also comparable to a_p for the xylene system. The interfacial areas in the lamellar region of the $E_{100}P_{70}E_{100}$−butan-1-ol−water system, 190−240 Å^2, are found to be higher than those for the hexagonal region; the biggest discrepancy is for the two 25% butanol samples where $a_p \approx 240$ Å^2. It is interesting to note that if a_p for these samples were calculated from eq 6 (valid for the hexagonal structure), then the obtained value would be 140 Å^2, which is at the low end of the 145−170 Å^2 range found in the hexagonal region. The structure of these two samples has been assigned as lamellar based in the presence of $1 \div 2 \div 3$ ... diffraction peaks and the absence of the $\sqrt{3}$, $\sqrt{7}$ peaks (expected for hexagonal structure); the discrepancy in the a_p values discussed above casts some doubts on this assignment.

Location of *n*-Butyl Acetate. The same procedure outlined above for butanol was also used in the butyl acetate case. Butyl acetate is more soluble in water than xylene, but less so than butanol, and we expect butyl acetate to participate both in the apolar and the interfacial regions. Two factors will determine the effective apolar and interfacial volume fractions. The first is the fraction, x, of butyl acetate which is located in the (apolar) core of the microdomains, and the second is the fraction, n, of the butyl acetate which contributes to the interfacial volume. This will give two expressions for the apolar, f_3, and interfacial, Φ_3, volume fractions:

$$f_3 = \Phi_{PPO} + x\Phi_{but\ acet} \quad (13)$$

$$\Phi_3 = \Phi_p + n\Phi_{but\ acet} \quad (14)$$

After testing a number of possible locations for butyl acetate against the idea that the interfacial area per copolymer molecule should be invariant of composition, we found that $n \approx 0.75$ and $x \approx 0.36$. These numbers indicate that 75% of the butyl acetate participates at the polar/apolar interface together with the copolymer, and that 36% is located in the apolar core of the "oil"-in-water microdomains. This 36% part resulted from the sum of the 25% $(1 - n)$ of butyl acetate which did not partition at the interface, and a contribution, 11%, to the apolar volume from the butyl acetate fraction (n) which is located at the interface (11% corresponds to 15% of $n \approx 0.75$−incidentally, this is comparable to 20% of $n = 1$ for the butanol case). The results from these considerations are presented in Tables 1 and 2. The interfacial area per PEO copolymer block is found in the range 125−150 Å^2 for the hexagonal region and 150−175 Å^2 for the lamellar region; a_p varies by about ±10% over the composition range examined.

Concerning the procedure which we used for obtaining Φ_{int} and f (based on the requirement that the interfacial area be roughly constant over the entire composition range of interest), we note that we did not pursue a rigorous minimization of the deviations of the interfacial area from a certain mean value, but we instead followed a trial and error approach (i.e., setting a number of different sets of Φ_{int} and f values and checking the resulting a_p). In this respect, there is still room for improvement in the Φ_{int} and f values which we present above as representative of the location of the different oils in the microdomains, but such refinement should not affect the conclusions of the present work. Small-angle neutron scattering (SANS) with contrast variation would be the more appropriate technique for obtaining the volume density profiles (and location of oil) in the microdomains.[30] Still, it is notable that such valuable information can be extracted from simple (and low capital cost) SAXS measurements.

Characteristic Lengths of Apolar Microdomains. The interfacial area per PEO block and the apolar cylinder radius values calculated (based on the procedures outlined above) for the normal hexagonal region of the three different phase diagrams, are plotted in parts a and b, respectively, of Figure 6 as a function of copolymer concentration. The interfacial area indeed remained almost constant (at 150−170 Å^2) throughout the wide composition range examined in both the butanol and xylene systems, as prescribed above. The interfacial area values in the butyl acetate system were a bit smaller (130−150 Å^2). All systems converge to the same interfacial value at high copolymer concentrations, because under these conditions the contribution of the "oil" to the determination of f and Φ diminishes.

The apolar cylinder radius, R, in the butanol system remained constant at 32 Å up to 40 wt % copolymer, and then gradually increased with increasing copolymer concentration, to reach a value of 38 Å. The xylene and butyl acetate system had a larger apolar cylinder radius (≈50 Å) than the butanol system; this is a consequence of the xylene being located in the core of the oil-in-water cylindrical assemblies.

The dependence on copolymer concentration of another length, b, characteristic to the hexagonal structure is shown in Figure 6c. b, equal to $2d/\sqrt{3} - 2R$, is the shortest distance between nearest-neighbor polar/apolar interfaces and corresponds to the smallest thickness of two overlapping (and interacting) PEO layers (d, R, and b are shown in the inset of Figure 6c). b decreases significantly (from ≈125 to ≈70 Å) with increasing copolymer volume fraction, indicating that the packing of the PEO chains in the domains between the cylinders becomes denser.

The trends followed by the characteristic lengths in the lamellar regions are not that clear, because of the narrower concentration range of the lamellar phases (and the correspondingly smaller number of SAXS measurements) and also because of the very different locations of the lamellar regions in the three phase diagrams. The calculated interfacial area per PEO

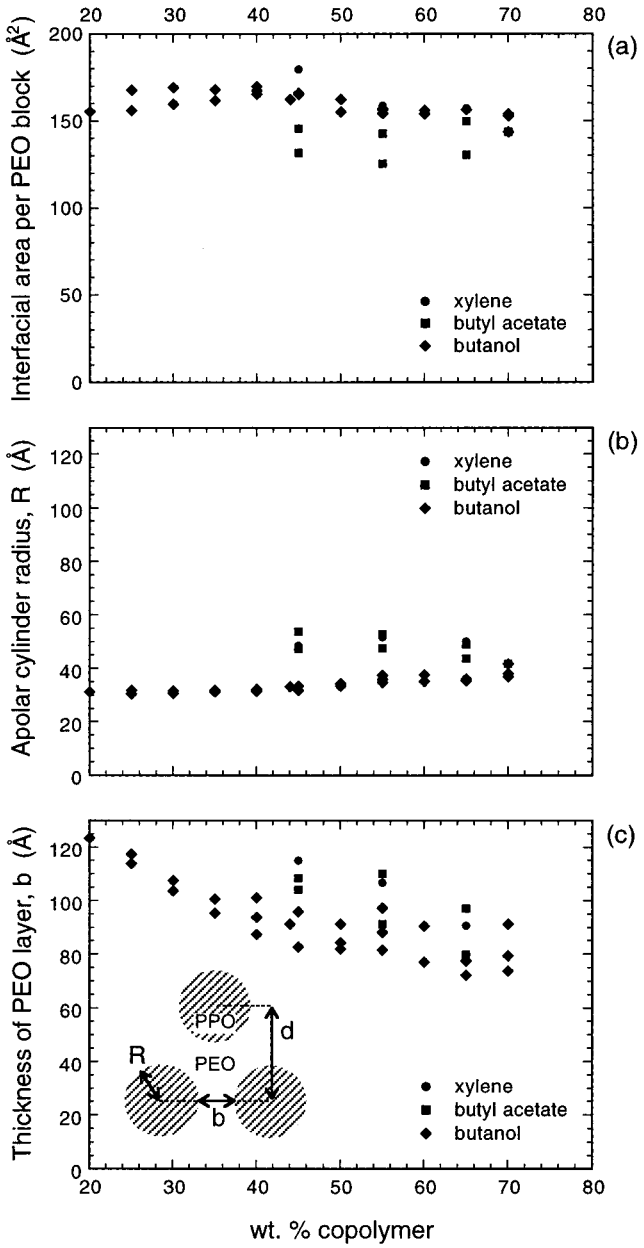

Figure 6. Values for (a) the interfacial area per PEO block, a_p, (b) the apolar cylinder radius, R, and (c) the shortest distance between nearest-neighbor polar/apolar interfaces (PEO layer thickness), b, presented as a function of wt % of $E_{100}P_{70}E_{100}$ in the normal hexagonal region for the three copolymer−oil−water systems: xylene (circles), butyl acetate (squares), and butanol (diamonds). A triangular section of the hexagonal structure is included in Part c to illustrate the various characteristic lengths.

chain and apolar lamellar thickness values are presented in Table 2. The apolar thickness values follow the expected trend: largest thickness for the xylene system and smallest for the butanol.

Summary and Conclusions

The present study focuses on the phase behavior and structure of ternary amphiphilic block copolymer−"oil"−water systems as affected by the "oil" type. We examined the same block copolymer, $E_{100}P_{70}E_{100}$, with three different "oils" of varying polarity, *p*-xylene, *n*-butyl acetate, and butan-1-ol. A large variety of phases is found in all three ternary systems, but the overall phase behavior (e.g., the number of phases and the composition range of their stability) depends on the "oil" used.

Butanol is unique in that it can stabilize lamellar and hexagonal ("gel") phases at low (down to 12 wt %) copolymer concentrations, and also the L_2 solution phase at high copolymer concentrations (up to 60 wt %). It thus acts in a manner comparable to cosurfactants known from systems containing low-molecular-weight amphiphiles. The normal hexagonal and the lamellar regions in the cases of butyl acetate and xylene are stable at copolymer concentrations above 45 wt %. Up to 30 wt % butyl acetate but only 10 wt % xylene can be accommodated in the normal hexagonal structure. The stability of the cubic structure from 20 up to 65 wt % copolymer concentration range and its ability to solubilize significant amounts of butanol and butyl acetate are notable, given its practical applications.

The characteristic length scales, e.g., nearest neighbor distance, bilayer thickness, and cylinder radius, in the different phases were determined from SAXS measurements. For the same ternary composition and structure, the lattice spacing was found to decrease as the "oil" became less hydrophobic (more polar), i.e., from xylene to butyl acetate to butanol. This trend was observed in both the normal hexagonal and the lamellar regions, and suggested a different location for the "oils".

The location of the "oil" in the different microstructures has been deduced from the structural dimensions obtained from SAXS and the constraints imposed by the total volume fraction of the copolymer and oil, and the consideration that the interfacial area per copolymer molecule be independent of the overall composition. We thus showed that all xylene is located in the interior (core) of the "oil"-in-water microdomains and none at the polar/apolar interface and butanol participates primarily in the interfacial volume and only slightly (about 20%) in the apolar volume, while butyl acetate contributes to both the total interfacial volume (by about 75%) and the apolar volume (about 36% of butyl acetate is located in the core).

Acknowledgment. Financial support from the Swedish Natural Science Research Council (NFR) and the Swedish Research Council for Engineering Sciences (TFR) is gratefully acknowledged. The acquisition of the SAXS apparatus in our laboratory was funded by the Swedish Council for Planning and Coordination of Research (FRN).

References and Notes

(1) Alexandridis, P.; Olsson, U.; Lindman, B. *Macromolecules* **1995**, *28*, 7700.
(2) Alexandridis, P.; Olsson, U.; Lindman, B. *J. Phys. Chem.* **1996**, *100*, 280.
(3) Alexandridis, P.; Olsson, U.; Lindman, B. *Langmuir* **1996**, *12*, 1419.
(4) Alexandridis, P.; Olsson, U.; Lindman, B. *Langmuir* **1997**, *13*, 23.
(5) Alexandridis, P.; Olsson, U.; Lindman, B. Submitted for publication.
(6) Alexandridis, P.; Zhou, D.; Khan, A. *Langmuir* **1996**, *12*, 2690.
(7) Alexandridis, P.; Holmqvist, P.; Lindman, B. *Colloids Surf. A*, in press.
(8) Holmqvist, P.; Alexandridis, P.; Lindman, B. *Langmuir* **1997**, *13*, 2471.
(9) Wanka, G.; Hoffmann, H.; Ulbricht, W. *Macromolecules* **1994**, *27*, 4145.
(10) Almgren, M.; Brown, W.; Hvidt, S. *Colloid Polym. Sci* **1995**, *273*, 2.
(11) Alexandridis, P.; Hatton, T. A. *Colloids Surf. A* **1995**, *96*, 1.
(12) Mortensen, K. *J. Phys.: Condens. Matter* **1996**, *8*, A103.
(13) Chu, B.; Zhou, Z. *Surf. Sci. Ser.* **1996**, *60*, 67.
(14) Schmolka, I. R. *J. Am. Oil Chem. Soc.* **1977**, *54*, 110.
(15) Edens, M. W. *Surf. Sci. Ser* **1996**, *60*, 185.
(16) Alexandridis, P. *Curr. Opin. Colloid Interface Sci.* **1996**, *1*, 490.

(17) Alexandridis, P. *Curr. Opin. Colloid Interface Sci.* **1997**, *2*, 478.
(18) Laughlin, R. G. *The Aqueous Phase Behavior of Surfactants*; Academic Press: London, 1994.
(19) Olsson, U.; Wennerström, H. *Adv. Colloid Interface Sci.* **1994**, *49*, 113.
(20) Bates, F. S.; Schulz, M. F.; Khandpur, A. K.; Förster, S.; Rosedale, J. H.; Almdal. K.; Mortensen, K. *Faraday Discuss.* **1994**, *98*, 7.
(21) Matsen, M. W.; Bates, F. S. *Macromolecules* **1996**, *29*, 1091.
(22) Malmsten, M.; Lindman, B. *Macromolecules* **1993**, *26*, 1282.
(23) Mortensen, K.; Talmon, Y. *Macromolecules* **1995**, *28*, 8829.
(24) Godward, J.; Heatley, F.; Booth, C. *J. Chem. Soc. Faraday Trans.* **1995**, *91*, 1491.
(25) Kirschner, E. M. *Chem. Eng. News* **1994**, *72*, (June 20), 13.
(26) Zana, R.; Eljebari, M. J. *J. Phys. Chem.* **1993**, *97*, 11134.
(27) Hahn, T., Ed. *International Tables for Crystallography*; D. Reidel Publishing Company: Dordrecht, The Netherlands, 1983; Vol. A.
(28) Fontell, K. *Colloid Polym. Sci.* **1990**, *268*, 264.
(29) von Erichsen, L. *Brennst.-Chem.* **1952**, *33*, 166.
(30) Chu, B. *Langmuir* **1995**, *11*, 414.

MA970625Q